

PROGRESS TOWARDS COMMISSIONING THE CORNELL DC FIELD DEPENDENCE CAVITY*

J. T. Maniscalco[†], T. Gruber, A. T. Holic, and M. Liepe
CLASSE, Cornell University, Ithaca, NY, 14853, USA

Abstract

The Cornell DC Field Dependence Cavity is a new coaxial test resonator designed to study the impact of strong (up to 200 mT or more) DC surface magnetic fields on the superconducting surface resistance, providing physical insight into the root of the “anti-Q-slope” and probing critical fields. In this report we report progress in the commissioning of this new apparatus, including finalized design elements and results of prototype tests.

INTRODUCTION

The microwave surface resistance of superconductors has been shown experimentally to depend on the strength of the RF magnetic fields parallel to the cavity surface [1]. While historically the surface resistance has most commonly been observed to increase with increasing field strength (*e.g.* in cavities with medium-field Q-slope and high-field Q-slope), recent results from nitrogen-doped and infused 1.3 GHz niobium cavities [2–4] as well as doped and clean niobium cavities at 2.6 and 3.9 GHz [5, 6] have demonstrated a surface resistance that *decreases* with increasing field strength, leading to extremely high intrinsic quality factors in an effect known as the “anti-Q-slope” or “positive Q-slope”. Further development of high- Q_0 cavities will greatly benefit from a fundamental understanding of this field dependence.

While these recent experiments have demonstrated the effects of time-varying magnetic fields, strong DC fields may have a similar effect on the surface resistance. Indeed, such a dependence has been observed experimentally in the past (see for example [7]), though in general these experiments did not probe bulk superconductors, or niobium specifically, or at frequencies or RF field levels relevant to modern SRF applications. The Cornell SRF group has developed the “DC Field Dependence Cavity” in order to measure this possible effect for contemporary SRF materials and frequencies. The cavity is now in the final phases of construction at Cornell, with commissioning forthcoming. Figure 1 shows an overview of the main components of the cavity.

Previous reports have given overviews of the principle of operation of the apparatus as well as initial and intermediate design considerations [8, 9]. Here we present a progress report for the cavity, detailing some final design changes as well as prototype test results of the superconducting electromagnet and the niobium-sapphire braze.

* This work was supported by the U.S. National Science Foundation under Award No. PHY-1549132, the Center for Bright Beams.

[†] jtm288@cornell.edu

DESIGN UPDATES

Since our last report on this cavity, we have made several finalizing changes to its design. The first of these was to modify the multipacting mitigation corrugations to further reduce multipacting effects. The corrugations and conical bore of the outer conductor serve to disrupt the normally severe multipacting bands in coaxial structures. While earlier designs featured ridges with semi-circular cross sections, after further simulation with Multipac [10] we found that rectangular corrugations were much more effective at reducing multipacting events. Figure 2 shows the cross-sectional geometry of the cavity with improved multipacting mitigation structures; Figure 3 shows some representative results of the multipacting simulations. For all three resonant modes, the improved corrugations eliminate low-order multipacting trajectories; all remaining multipacting trajectories are of high order ($N > 10$), indicating significantly reduced risk.

The second design change in the finalization was a modification to the dimensions of the superconducting magnet. This was necessary to correct for an error in the dimensions of the stock of superconducting NbTi wire, which was oversized in diameter by $\sim 5\%$ in comparison to the specification. This discrepancy was first detected in the prototype magnet test (see below for these results). The changes to the design amounted to slight modifications to the width and depth of the steps in the magnet’s mandrel, designed by genetic algorithm for enhanced field uniformity along the axis of the solenoid. We re-optimized the mandrel geometry using the genetic algorithm routine given the corrected wire diameter, yielding deeper steps with subtly different widths.

PROTOTYPE MAGNET TEST

A major component of the design of the apparatus is the superconducting electromagnet situated coaxially with the resonant cavity. As mentioned above, genetic algorithm optimization was used to design “steps” in the mandrel of the magnet, sections with decreased radius allowing for extra wire turns to correct for fringe field errors. Figure 4 shows a cross-sectional view of the mandrel. We built a miniature prototype magnet to test the efficacy of this design technique, in particular looking to see that the steps improved uniformity and that the step edges did not introduce any shorts in the superconducting wires by cutting through the insulation. Figure 5 shows this prototype.

Figure 6 shows the results of the warm and cold tests of the magnet prototype alongside the theoretical prediction. While the measurements indicate high uniformity near the center of the solenoid, the fringe fields taper earlier than

Content from this work may be used under the terms of the CC BY 3.0 licence (© 2019). Any distribution of this work must maintain attribution to the author(s), title of the work, publisher, and DOI.

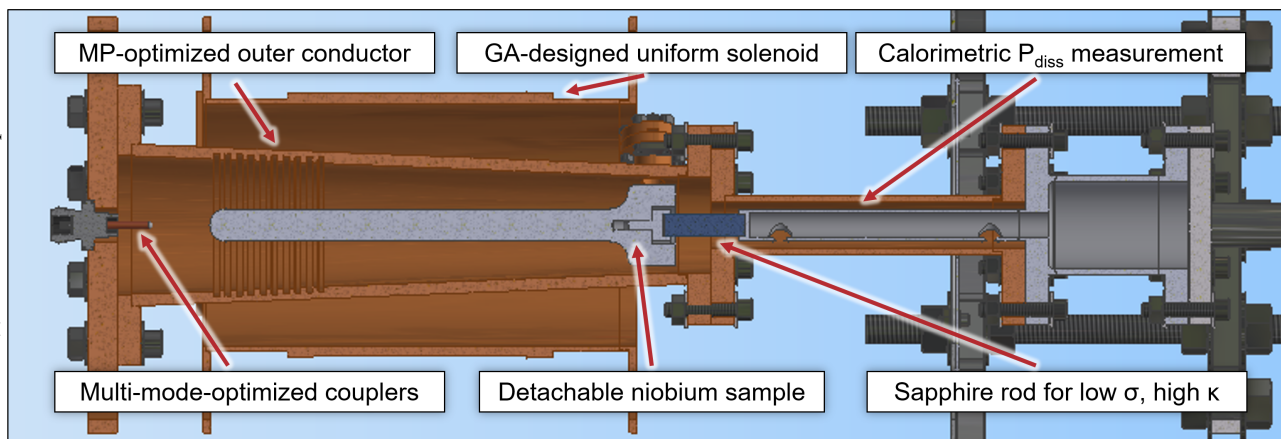


Figure 1: Overview CAD image of the DC Field Dependence Cavity.

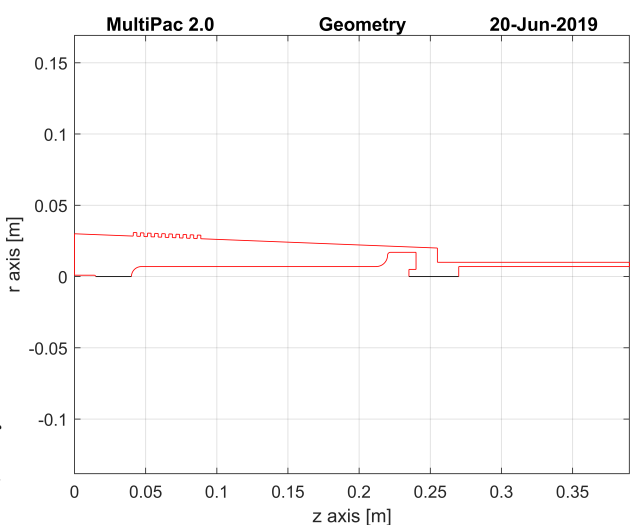


Figure 2: Cross-sectional geometry of the DC Field Dependence Cavity featuring improved multipacting mitigation corrugations.



Figure 4: Cross section of the mandrel of the superconducting solenoid, featuring GA-optimized steps for improving field uniformity.



Figure 5: Prototype magnet.

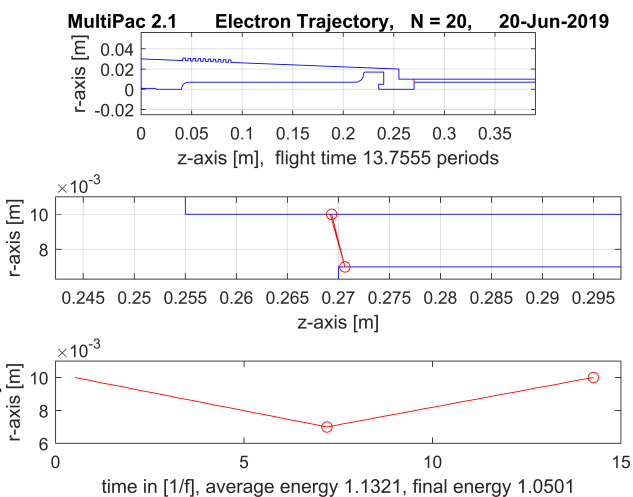


Figure 3: Simulations yield extremely limited multipacting; remaining multipacting trajectories (such as the one pictured here) are in general high-order.

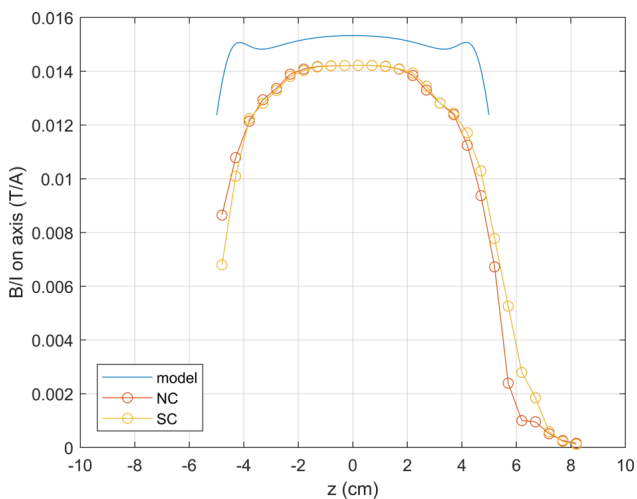


Figure 6: Comparison of results of warm and cold test of the prototype solenoid to the theoretical model. Discrepancies are likely due to incorrect wire diameter, and will be corrected for in the final design.

expected compared to the model. In addition, the overall field level is $\sim 5\%$ lower than expected from simulation. We measured the diameter of the wire used to wind the solenoid and found that it was $\sim 5\%$ larger than the specification, causing a decreased winding density and therefore decreased field strength. We believe that this off-spec diameter is also responsible for the early tapering of the fringe fields: fewer wire layers fit into the steps than originally planned for, so the corrective effect of the step sections is reduced.

As mentioned above, this discrepancy has been accounted for in the final solenoid design. Tests of the final electromagnet will be presented in a future publication.

Comparing the results of the warm (normal-conducting) and cold (superconducting) tests of the prototype electromagnet, we find good agreement and left-right symmetry, indicating that there are no shorts between the wires and mandrel. This is a promising result for the principle of design of the mandrel steps.

PROTOTYPE SAPPHIRE BRAZE RESULTS

Essential to the cavity structure is the sapphire rod located centrally between the exchangeable inner conductor sample and the “thermal rod” used for the calorimetric measurements of dissipated power. The sapphire rod serves to electrically isolate the superconducting inner conductor sample from the rest of the cavity in order to prevent propagation of RF power down the thermal rod, as well as to thermally connect the inner conductor and thermal rod to allow for the calorimetric measurements. Sapphire in particular is desirable due to its good thermal conductivity [11] as well as its extremely low loss tangent at cryogenic temperatures, essential for minimizing unwanted RF losses [12]. In order to ensure good thermal connection and mechanical stability, the sapphire piece will be brazed to the niobium thermal rod and to a niobium-titanium screw for attaching the superconducting inner conductor.

Since the double braze of the sapphire piece to niobium and niobium-titanium is not a typical procedure in the Cornell SRF group’s brazing facilities, we sought to make a prototype braze joint using a full-size sapphire piece and dummy Nb and NbTi pieces. For the braze filler we used .003”-thick Nicoro (BAu-3), an off-the-shelf gold braze material with liquidus and solidus temperatures of 1000 and 1030 °C. In addition, we chemically prepared the sapphire with the procedures outlined in [13] in order to make the prototype braze as similar to the final braze as possible. These chemical procedures are necessary for minimizing the loss tangent of the sapphire piece.

We based the temperature profile of the braze on the “standard” recipe outlined in the literature [14]. Due to constraints in our vacuum braze furnace, we were unable to follow the recipe directly but instead followed a slightly modified temperature profile. The braze was performed in vacuum at the 1×10^{-9} Torr level, with the following temperature profile:

1. Ramp to 500°C (15 mins)

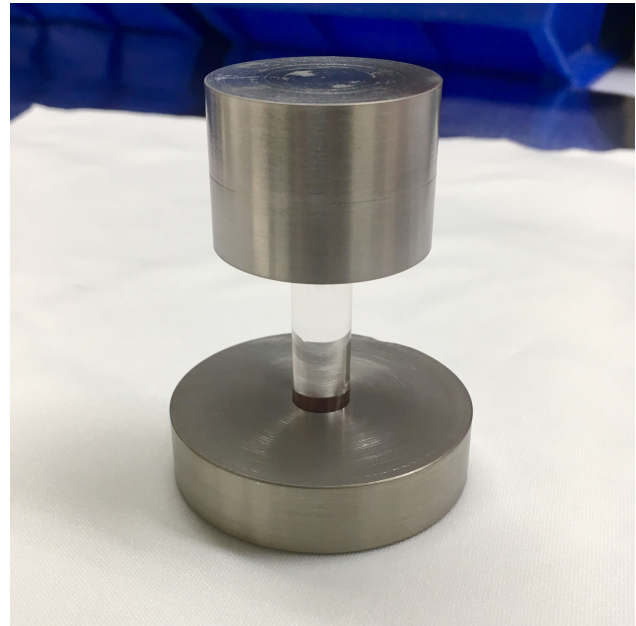


Figure 7: Prototype sapphire braze structure, with central sapphire crystal, upper NbTi piece, and lower Nb piece. For scale, the NbTi piece is 3.5 cm in diameter and 2.5 cm tall.

2. Equilibrate at 500°C (1 hr)
3. Ramp to 850°C (5 mins)
4. Equilibrate at 850°C (1 hr)
5. Ramp to 980°C (5 mins)
6. Equilibrate at 980°C (30 mins)
7. Ramp above liquidus to 1060°C (5 mins)
8. Soak above liquidus at 1060°C (35 mins)
9. Ramp back to room temperature

An initial test braze with a shorter final soak step (~ 5 mins) was only partially successful: the upper joint (NbTi-sapphire) was formed successfully, but the lower joint (Nb-sapphire) did not fully melt and as a result showed very poor tensile strength. With the longer soak step outlined above, the full structure shows good tensile strength and rigidity. Figure 7 shows a photograph of the finished braze prototype structure. The success of this braze gives great promise for the final cavity.

CONCLUSIONS

We have presented progress towards commissioning of the Cornell DC Field Dependence Cavity, highlighting some final design changes to reduce multipacting and to improve the uniformity of the DC magnetic field. We have shown results from a prototype of the superconducting solenoid, showing decent field uniformity and offering information useful for improving uniformity in the final electromagnet. We have also shown positive results of a prototype Nb-sapphire-NbTi double braze, exhibiting promise for the braze in the production cavity.

REFERENCES

- [1] H. Padamsee, J. Knobloch, and T. Hays. *RF Superconductivity for Accelerators*. Wiley-VCH, 2008.
- [2] A. Grassellino *et al.*, “Nitrogen and argon doping of niobium for superconducting radio frequency cavities: a pathway to highly efficient accelerating structures”, *Supercond. Sci. Technol.* vol. 26 p. 102001, 2013. doi:10.1088/0953-2048/26/10/102001
- [3] A. Grassellino *et al.*, “Unprecedented quality factors at accelerating gradients up to 45MVm^{-1} in niobium superconducting resonators via low temperature nitrogen infusion”, *Supercond. Sci. Technol.* vol. 30, p. 094004, 2017. doi:10.1088/1361-6668/aa7afe
- [4] P. N. Koufalas, F. Furuta, J. J. Kaufman, and M. Liepe, “Impact of the Duration of Low Temperature Doping on Superconducting Cavity Performance”, in *Proc. SRF’17*, Lanzhou, China, Jul. 2017, pp. 750–753. doi:10.18429/JACoW-SRF2017-THPB004
- [5] M. Martinello, M. Checchin, A. Romanenko, A. Grassellino, S. Aderhold, S. K. Chandrasekeran, O. Melnychuk, S. Posen, and D. A. Sergatskov, “Field-enhanced superconductivity in high-frequency niobium accelerating cavities”, *Phys. Rev. Lett.*, vol. 121, p. 224801, Nov 2018. doi:10.1103/PhysRevLett.121.224801
- [6] P. N. Koufalas, M. Liepe, J. T. Maniscalco, and T. E. Osieroff, “Experimental Results on the Field and Frequency Dependence of the Surface Resistance of Niobium Cavities”, in *Proc. IPAC’18*, Vancouver, Canada, Apr.-May 2018, pp. 2451–2454. doi:10.18429/JACoW-IPAC2018-WEPMF039
- [7] S. Sridhar and J. E. Mercereau, “Nonequilibrium dynamics of quasiparticles in superconductors”, *Phys. Rev. B: Condens. Matter*, vol. 34, pp. 203–216, July 1986. doi:10.1103/physrevb.34.203
- [8] J. T. Maniscalco, M. Liepe, and R. D. Porter, “Design Updates on Cavity to Measure Suppression of Microwave Surface Resistance by DC Magnetic Fields”, in *Proc. SRF’17*, Lanzhou, China, Jul. 2017, pp. 754–758. doi:10.18429/JACoW-SRF2017-THPB005
- [9] J. T. Maniscalco and M. Liepe, “Updates on the DC Field Dependence Cavity”, in *Proc. IPAC’18*, Vancouver, Canada, Apr.-May 2018, pp. 2465–2467. doi:10.18429/JACoW-IPAC2018-WEPMF044
- [10] P. Ylä-Oijala and D. Proch, “Updates on the DC Field Dependence Cavity”, in *Proc. SRF’01*, Tsukuba, Japan, Sep. 2001, pp. 105–107. <http://accelconf.web.cern.ch/AccelConf/srf01/papers/fa001.pdf>
- [11] M. W. Wolfmeyer and J. R. Dillinger, “The thermal conductivity of sapphire between 0.4 and 4°K ”, *Phys. Lett. A*, vol. 34, pp. 247–248, March 1971. doi:10.1016/0375-9601(71)90853-X
- [12] S. N. Buckley, P. Agnew, and G. P. Pells, “Cryogenic dielectric properties of sapphire at 2.45 GHz”, *J. Phys. D: Appl. Phys.*, vol. 27, pp. 2203–2209, Oct. 1994. doi:10.1088/0022-3727/27/10/033
- [13] N. J. Pogue, “Dielectric-Loaded Microwave Cavity for High-Gradient Testing of Superconducting Materials”, Ph.D. thesis, Texas A&M University, August 2011.
- [14] C. A. Walker, F. R. Trowbridge, and A. R. Wagner, “Direct brazing of sapphire to niobium”, *Welding Journal*, vol. 89, pp. 50–55, Mar. 2010.